



HAL
open science

Local Approach of the Charpy Test at Low Temperature

A. Rossoll, M. Tahar, C. Berdin, P Forget, R. Piques, C. Prioul, B. Marini

► **To cite this version:**

A. Rossoll, M. Tahar, C. Berdin, P Forget, R. Piques, et al.. Local Approach of the Charpy Test at Low Temperature. *Journal de Physique IV Proceedings*, 1996, 06 (C6), pp.C6-279-C6-286. 10.1051/jp4:1996627 . jpa-00254455

HAL Id: jpa-00254455

<https://hal.science/jpa-00254455>

Submitted on 4 Feb 2008

HAL is a multi-disciplinary open access archive for the deposit and dissemination of scientific research documents, whether they are published or not. The documents may come from teaching and research institutions in France or abroad, or from public or private research centers.

L'archive ouverte pluridisciplinaire **HAL**, est destinée au dépôt et à la diffusion de documents scientifiques de niveau recherche, publiés ou non, émanant des établissements d'enseignement et de recherche français ou étrangers, des laboratoires publics ou privés.

Local Approach of the Charpy Test at Low Temperature

A. Rossoll, M. Tahar*, C. Berdin, R. Piques*, P. Forget**, C. Prioul and B. Marini**

Ecole Centrale de Paris, Laboratoire MSS-MAT, URA 850 du CNRS, Grande Voie des Vignes, 92295 Châtenay-Malabry cedex, France

** Ecole des Mines de Paris, Centre des Matériaux, URA 866 du CNRS, BP. 87, 91003 Evry cedex, France*

*** CEA Saclay, CEREM, SRMA, 91191 Gif-sur-Yvette cedex, France*

Abstract : Charpy V-notch impact testing is widely used in the toughness assessment of large forged components, e.g. the pressure vessel for pressurised water reactors (PWR). At low temperature, A508 Cl.3 nuclear pressure vessel steel fails by cleavage fracture. The results reported here are part of both an experimental program and numerical investigations which aim at the establishment of a non-empirical relationship between the lower shelf Charpy V-notch energy, CVN, and the fracture toughness, K_{Ic} , of this material. Here, the applicability of the Beremin cleavage fracture model to the Charpy specimen is demonstrated.

1. INTRODUCTION

Both fracture toughness (e.g. CT) and Charpy impact tests are used for the characterisation of the fracture behaviour of structural steels. The Charpy impact test is frequently employed in order to qualify the state of brittleness of a material, since it is very easy to conduct and requires only small specimens ($10 \times 10 \times 55 \text{ mm}^3$). However, the determination of an intrinsic K_{Ic} value from Charpy tests is questionable. For example, it is not clear if the cleavage strength is independent of dynamic effects (oscillations, high strain rates, local temperature rises etc.). Furthermore, the state of constraint is different in Charpy and fracture mechanics specimens. Up to now, the correlations between a material's fracture toughness (K_{Ic}) and its Charpy V-notch impact energy (CVN) are empirical. Some of these correlations are listed in [1] and [2]. No unique correlation can cover the entire transition range. The present work is part of more extensive experimental and numerical investigations which aim on the determination of a better founded relationship between lower shelf CVN and K_{Ic} for an A508 Cl.3 bainitic nuclear pressure vessel steel. In this paper, as a first step, the applicability of a local approach by using the Beremin model [3] to the Charpy specimen is examined.

Beremin applied the model to axisymmetric notched tensile bars of various notch radii, and to four point bend specimens. By its application to the crack tip situation, the authors established a link between the local parameters of the model and the "global" value of fracture toughness. The model is based on the existence of a temperature-independent critical cleavage stress. Plastic deformation induces the nucleation of micro-cracks which are generally oriented normal to the direction of the maximum principal stress σ_1 . Instability (failure of the entire specimen) occurs when σ_1 reaches a critical stress in a representative volume. The weakest link theory assumes that these representative volume elements are independent one from each other. Using a power law distribution for the size of the micro-cracks, the Beremin criterion can be expressed in the following statistical form :

$$P_r = 1 - e^{-\left(\frac{\sigma_w}{\sigma_u}\right)^m} \tag{1}$$

with

$$\sigma_w = \sqrt[m]{\int_{V_{pl}} \sigma_1^m \frac{dV}{V_0}} \tag{2}$$

where P_r (eq. 1) is the cumulative failure probability, and σ_w (eq. 2) the Weibull stress (summation function of σ_1 on the plastically deformed volume V_{pl}). V_0 (eq. 2) is a characteristic volume of the material, V_0 is chosen as a cubic volume containing several grains (8 in the original paper [3]). Here, $V_0 = (50 \mu\text{m})^3$. σ_u is closely linked to the intrinsic cleavage stress and m is the Weibull exponent which describes the scatter in the flaw distribution. Two parameters are required : m and $V_0 \sigma_u^m$.

Normalised Charpy V-notch specimens ($10 \times 10 \times 55 \text{ mm}^3$, 2 mm deep notch) were tested at low temperature on an instrumented pendulum impact machine. The Weibull statistics parameters m and σ_u are identified using two specimen geometries : Charpy V-notch specimens and axisymmetric notched tensile bars.

2. MATERIAL AND MECHANICAL BEHAVIOUR

2.1 Material

Two similar heats of a low alloy carbon steel widely used for nuclear constructions (A508 Cl.3) were tested. Heat A is a representative sample of the inner part of a pressure vessel wall and heat B was taken from a nozzle cut-out of another pressure vessel. The chemical composition is given in table 1.

Table 1 : Chemical composition (wt.%) :

	C	S	P	Si	Mn	Ni	Cr	Mo	Cu
Heat A	0.16	0.004	0.008	0.22	1.33	0.76	0.22	0.51	0.07
Heat B	0.159	0.008	0.005	0.24	1.37	0.70	0.17	0.50	0.06

Heat treatment for both materials consisted of two austenitisations, followed by water quenching and tempering, and a final stress relief. The resulting microstructure was tempered upper bainite with an average grain size of about $20 \mu\text{m}$. The orientation of the specimens tested and the yield strength of the two heats are reported in table 2.

Table 2 : Specimen orientation :

Specimen	Heat A	Heat B
smooth tensile/compressive	Y (T)	Y (T)
notched axisymmetric	X (L)	Y (T)
Charpy V-notch	Y-X (T-L)	Y-Z (T-S)
$R_{p0.2}$ at room temperature (MPa)	492	516
$R_{p0.2}$ at -100°C (MPa)	573	627

2.2 Mechanical behaviour

The material just below the notch root of the Charpy specimen undergoes high strain-rate deformation during the test. Therefore the strain-rate sensitivity of the material has to be taken into account. Thus the uniaxial flow properties have been investigated under both static and dynamic loading conditions, in a wide range of temperatures [-196°C to $+100^\circ\text{C}$]. The determination of the yield stress σ_y and the hardening parameters was carried out in tension at $\dot{\epsilon} \sim 10^{-4} \text{ s}^{-1}$ and $\dot{\epsilon} \sim 50 \text{ s}^{-1}$ for heat A [4]. Additional compressive tests at $\dot{\epsilon} \sim 1000 \text{ s}^{-1}$ were performed on heat B by means of a Hopkinson bar device. Similar characteristics were found for both heats, except that heat B shows stronger strain hardening.

The Cowper-Symonds elastic-viscoplastic formulation (eq.3) implemented in ABAQUS [5] has been applied in order to incorporate strain-rate effects.

$$\sigma = \sigma_0 \left(1 + \left(\frac{\dot{\epsilon}_{eq}}{\dot{\epsilon}_0} \right)^{1/p} \right) \quad (3)$$

where

- σ : dynamic flow stress
- σ_0 : static flow stress (for each temperature of interest)
- $\dot{\epsilon}_{eq}$: equivalent plastic strain rate
- $\dot{\epsilon}_0$: normalisation parameter
- p : strain rate hardening exponent

The static flow stress for strains greater than the uniform tensile strain was obtained by extrapolation of the hardening curve during the last 5% of strain prior to necking. The parameters $\dot{\epsilon}_0$ and p were fitted numerically.

3. EXPERIMENTAL PROCEDURE AND RESULTS

3.1 Experimental procedure

Charpy V-notch tests with a nominal impact velocity of 5 m/s were carried out in a temperature range of [-196°C to +100°C] on a standard pendulum impact machine of 350 Joules capacity. The instrumented striker allows the recording of the evolution of load vs. time. The reliability of the instrumentation can be assessed by comparing the calculated energy with the impact energy read from the machine dial. The axisymmetric notched tensile bars were tested on a servohydraulic testing machine at a crosshead speed of 0.25 mm/min.

3.2 Results

When impact specimens fail after very short loading times due to their brittle behaviour, the presence of strong inertial effects needs to be accounted for in evaluation of results. The load-time record of an impacted specimen shows strong inertial oscillations over the test duration. Inertia can be so predominant that very brittle specimens can be tested without the use of supports. This is the case in one-point testing, where the specimen is entirely loaded by inertia [6]. A more conventional and more universal approach in the time domain of strong inertial effects is the evaluation of conventional three point bend tests (e.g. Charpy) via dynamic key impact response curves which directly yield K_{Id} (dynamic fracture toughness) values, as suggested by Böhme [7] and Kalthoff [8]. However, this method requires the use of precracked specimens. It is more often employed for testing large bend specimens, where dynamic effects do not dampen out quickly due to spreading plasticity.

By experimental evidence (comparison of measured tup loads for impacted supported and unsupported specimens) Server [1, 9] established a criterion for applying a quasistatic evaluation procedure. His conservative recommendation for a validity limit is a minimum time to fracture of three apparent oscillations ($\tau = 3$) on the load-time record. However, our own FEM computations [10] indicate that a time $\tau = 2$ could be considered sufficient in order for the kinetic energy of the specimen to become very small in comparison with its elastic and plastic strain energy. Additionally, local stresses in the highly strained notch root region (where failure initiates) were investigated. They show almost no oscillations, since plasticity develops very early in the load-time history and has a strong dampening effect.

In figure 1 the evolution of Charpy V-notch impact energy with temperature is reported for heats A and B

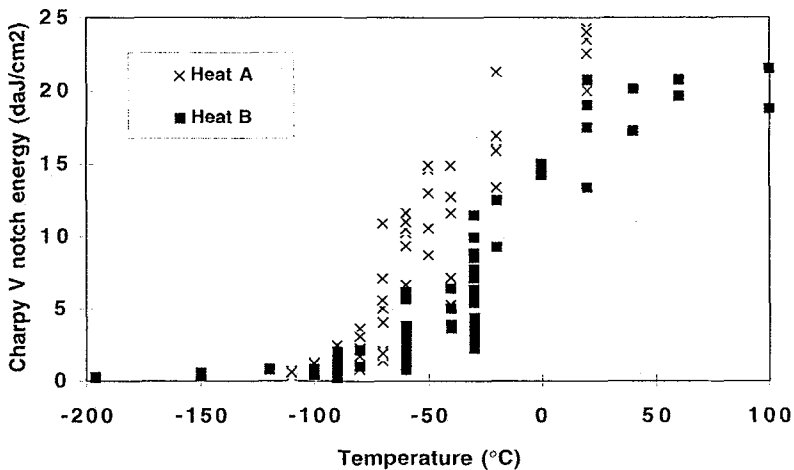


Figure 1 : Charpy V notch energy vs. temperature for heats A and B.

respectively. Heat B is found to be slightly more brittle in terms of DBTT (ductile-to brittle transition temperature) than heat A. In terms of 7 daJ/cm^2 Charpy V-notch impact energy, the transition temperatures are -60°C and -30°C respectively. For the Charpy specimens tested in the cleavage domain at $T = -90^\circ\text{C}$, at least two periods of oscillations could be observed prior to failure. According to the discussion above, a quasistatic evaluation procedure is justified. Figure 2 illustrates a typical load vs. displacement curve (heat A ; -80°C), in comparison with “dynamic” and “quasistatic” computed curves (see § 4.1). Fracture surface observations showed no stable ductile crack initiation at temperatures below -70°C .

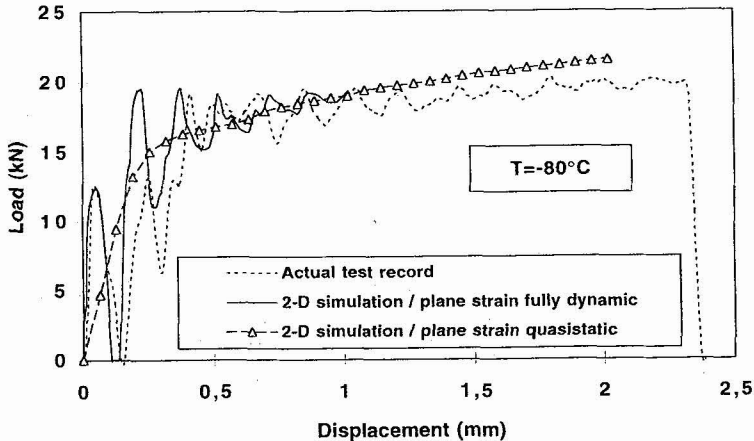


Figure 2 : Comparison of measured and computed load-displacement curves.

4. NUMERICAL COMPUTATIONS

4.1 Numerical procedures

For the Charpy specimen, a “fine” and a “coarse” 2-D mesh as well as a “coarse” 3-D mesh have been designed. In 2-D, only one half of the specimen needs to be modelled. The “fine” mesh consists of 2300 four-noded linear isoparametric elements with reduced integration. The element size just below the notch root is of the order of $30 \mu\text{m}$. Plane strain conditions have been assumed. The 3-D mesh for one quarter of the specimen (see figure 5) is composed of 8700 eight-noded linear isoparametric elements with reduced integration. The smallest element size is $50 \times 100 \times 250 (\mu\text{m})^3$. The “coarse” 2-D mesh is characterised by the same resolution as the 3-D mesh.

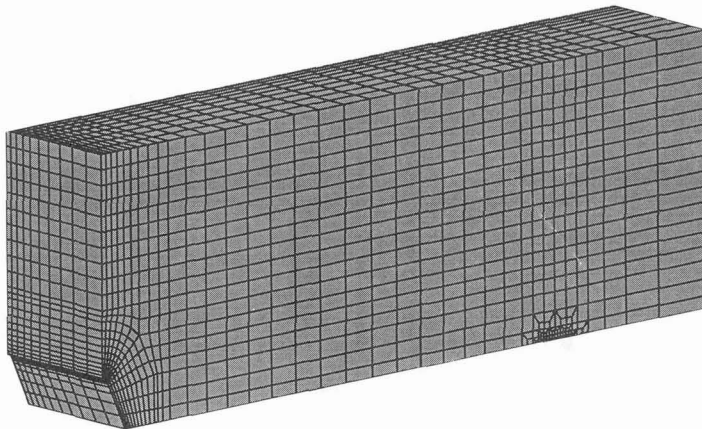


Figure 3 : 3-D mesh of one-quarter of the Charpy-V notch specimen (not showing the analytical contact surfaces modelling the striker and the anvil).

For all models, the mesh is locally refined for modelling the surfaces in contact with the striker and the anvil (prescribed as rigid analytical contact surfaces), allowing a good description of specimen indentation. Loading is modelled by prescribing the velocity of the striker contact surface reference node. For further details see Refs [10] and [11].

The axisymmetric notched specimen geometry has been modelled with axisymmetric elements.

In order to be able to conduct quasistatic as well as fully dynamic (including inertia terms) analyses, we chose the ABAQUS code [5]. A large deformation formulation is used. As it has been emphasised in §2.2, the material can be considered as elastic-viscoplastic with isotropic hardening. Table 3 sums up the FEM calculations for the Charpy specimen.

Table 3 : Numerical computations :

Heat	Mesh	Solution procedure	Material law
A and B	2-D plane strain	static = not incorporating inertial effects	elastic-viscoplastic
A and B	2-D plane strain	dynamic = incorporating inertial effects	elastic-viscoplastic
B	3-D	static = not incorporating inertial effects	elastic-viscoplastic

4.2 Results

Figure 2 shows a comparison of an actual Charpy test record together with simulated load vs. displacement curves obtained by quasistatic and fully dynamic 2-D plane strain calculation. For this typical test (heat A, -80°C), the modelling of the oscillation regime is in good agreement with the experimental data. A better fit for the period of apparent oscillations was obtained by modelling the machine compliance via a spring element between the striker contact surface reference node and the node for which the striker movement is prescribed as a boundary condition. For displacements exceeding 0.5 mm, inertial oscillations are largely damped due to spreading plasticity. This damping effect has been found to be even more pronounced for local stresses just below the notch root. Thus a quasistatic computing procedure (i.e. neglecting inertial terms) is considered a quite satisfactory approach to model unstable fracture in this material at low temperature. More attention however needs to be paid to simulate tests at even lower temperature (less than -120°C for example), see also the discussion in §3.2.

For displacements exceeding 1 mm, the 2-D plane strain simulation overestimates the load-displacement curve. This tendency would exist even if ductile damage were taken into account. For the 3-D model a very good agreement between experimental and computed global response curves was found [10]. Since dynamic analysis would be numerically very expensive in 3-D, and has finally been judged unnecessary in the time domain investigated, only quasistatic 3-D computations have been carried out.

The evolution of the largest principal stress (σ_1) along the ligament, obtained by plane strain quasistatic analysis, is plotted in figure 4, for increasing specimen deflection. It can be observed that the peak value of

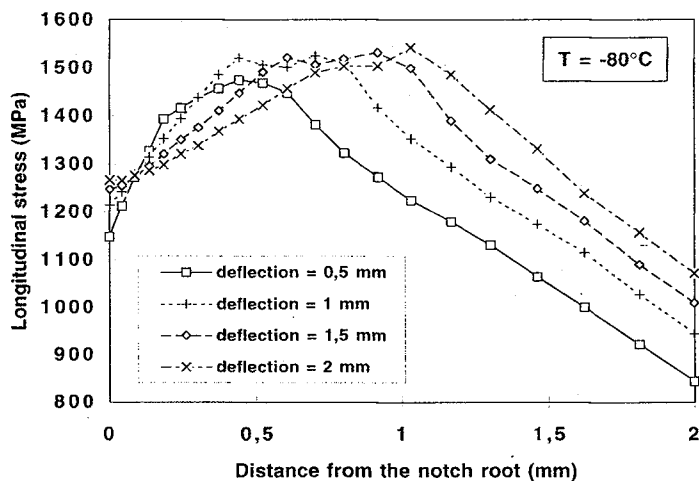


Figure 4 : Evolution of the longitudinal tensile stress during the test (2-D quasistatic plane strain calculation).

this tensile stress is shifted from 0.5 to 1 mm. Referring to the notch root radius ($\rho = 0.25$ mm), the shift range is $[2\rho$ to $4\rho]$. In heat A, which exhibits little strain hardening, this peak value does not increase. For heat B, which shows a stronger strain hardening behaviour, tensile stresses increase considerably. For both heats, a broadening of the peak value of tensile stress is observed. This means that, for increasing load, a larger material volume is subjected to high stresses, which increases fracture probability, see § 5. Recent investigations (reported in [10]) concerning a comparison of isothermal and adiabatic conditions show that adiabatic heating is closely confined to the notch root. Consequently, its influence on the peak tensile stress can be neglected.

5. LOCAL APPROACH

The experimental results are analysed in terms of the Beremin model [3], which is applied in a post-processing routine. The Weibull statistics parameters m and σ_u have been identified for two specimen geometries : axisymmetric notched tensile bars (heats A and B) and Charpy V-notch specimens (heat B only).

5.1 Axisymmetric notched tensile bars

To follow the original Beremin procedure [3] for heat A, 19 axisymmetric notched tensile bars AE-2 and AE-4 (minimum diameter $r_0 = 6$ mm, root radius $\rho = 1.2$ or 2.4 mm) were tested at -196°C and -160°C respectively under static strain rate conditions ($\dot{\epsilon} \sim 10^{-4} \text{ s}^{-1}$). Finite element calculations of the Weibull stress σ_w (eq. 2) as a function of the stress and deformation fields were made using the Zebulon code which has been developed at Ecole des Mines de Paris. The details of both experimental and numerical investigations are presented elsewhere [11]. The iterative identification of m and σ_u is based on the linear correlation between $\text{Ln}(\text{Ln}(1/(1-P_f)))$ and $\text{Ln}(\sigma_w)$ (see eq. (1)). The parameters obtained by this procedure can be found in table 4.

For heat B, 35 axisymmetric tensile specimens AE-2 were tested at -150°C . FEM analyses were conducted with ABAQUS. The Weibull parameters have been identified by means of the maximum likelihood iterative method [12].

Specimens have been ranked in terms of displacement (reduction of diameter) at failure. Fracture probability vs. Weibull stress is plotted in figure 5 for heats A and B.

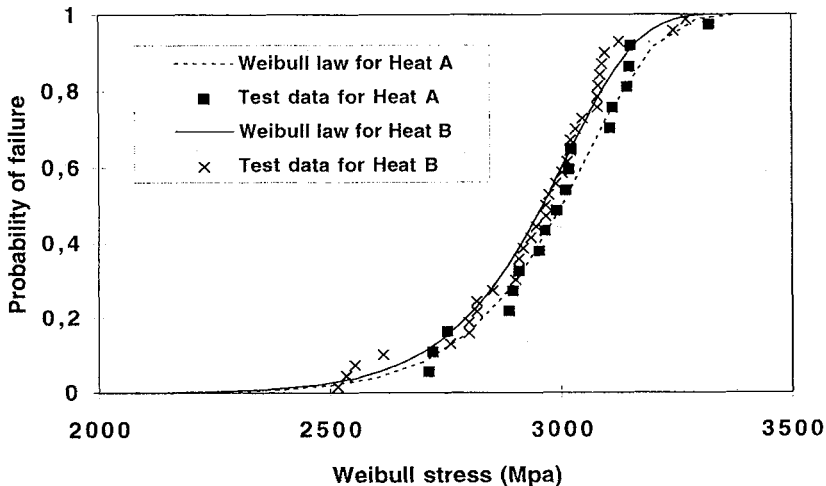


Figure 5 : Beremin model applied to axisymmetric notched specimens of heats A and B.

5.2 Charpy V-notch specimens

In this case, 2-D and 3-D quasistatic modelling (elastic viscoplastic material behaviour) was used. The

Weibull stress σ_w was computed for 28 Charpy V-notch specimens tested at -90°C (see figure 6). Specimens have been ranked in terms of deflection at failure (between 0.28 and 1.04 mm). A maximum likelihood iterative method [12] is applied for the identification of the parameters m and σ_u .

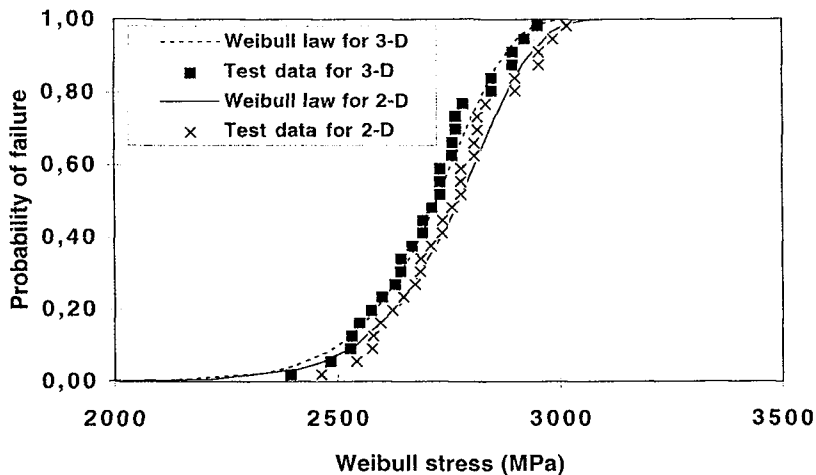


Figure 6 : Beremin model applied to Charpy V notch specimen of heat B, 2-D “coarse” mesh and 3-D simulation.

5.3 Comparison

Table 4 sums up the Weibull parameters obtained. The term $\sigma_u V_0^{1/m}$ is included for better comparison of different heats, geometries, temperatures, etc., since m and σ_u are interdependent.

Table 4 : Weibull parameters obtained :

Heat	Specimen orientation	Specimen type	FEM-model	Number of specimens	m	σ_u (MPa)	$\sigma_u V_0^{1/m}$
A	X	AE-2 and AE-4	axisymmetric	19	20	3059	1952
B	Y	AE-2	axisymmetric	35	19	3142	1937
B	Y-Z	CVN	2-D plane strain fine mesh	28	22	2806	1865
B	Y-Z	CVN	2-D plane strain coarse mesh	28	22	2821	1867
B	Y-Z	CVN	3-D	28	22	2769	1849

The following observations can be made :

As has already been shown in figure 1, heat A is characterised by a lower DBTT, and a higher upper shelf impact energy value. This is consistent with the fact that both its yield strength is lower, and strain hardening is less pronounced. However, the cleavage strength does not seem to be effected, since the computed values of σ_u and m lie very close.

2-D “fine” and “coarse” mesh results on the Charpy specimen lie very close to each other, which means that, in this case, the Beremin model is almost mesh-insensitive for reasonable mesh-sizes. This is not surprising, since stress gradients ahead of the relatively smooth notch of the Charpy specimen are weak compared to the situation ahead of cracks (e.g. compact tension specimen). The computationally much more expensive 3-D model yields parameters which lie very close to those obtained in 2-D. Consequently a 2-D model can be considered sufficiently accurate. This point is confirmed by fractographic observations that prove that fracture usually initiates in the centre of the specimen, where stresses are high and a plane strain assumption is well justified.

A deviation of less than 10 % is found when comparing the Weibull parameters obtained on axisymmetric tensile specimens with those computed for Charpy specimens. This effect might be due to some slight

temperature or strain-rate dependence of the material's "intrinsic" cleavage stress. Additional test data would be necessary in order to examine this observation. Further work, that incorporates stable ductile crack growth, is also necessary for the examination of the ductile-to-brittle transition (higher temperatures than those investigated here).

"Key curves", as presented in [13] could be established, in order to allow easy computation of Weibull parameters for the Charpy specimen. Of course, these key curves would need to take into account the strain rate sensitivity of the material.

More work is required before a new relationship between Charpy V-notch Energy CVN and fracture toughness K_{Ic} can finally be proposed.

6. CONCLUSIONS

- 1) The application of the Beremin model to the Charpy test yields reasonable values for the Weibull parameters. The Weibull parameters obtained deviate by less than 10% from those obtained for a different geometry, strain rate and temperature, i.e. with those obtained with the "classical" axisymmetric notched tensile specimen.
- 2) A simple 2-D quasistatic FEM model of the instrumented Charpy impact test is sufficient for application of the Beremin model at relative low temperature (cleavage domain).
- 3) Consequently, "key curves" could be established, which provide a simple method for correlating loadpoint deflection at failure with failure probability for the Charpy test.
- 4) These conclusions are only valid in the pure cleavage domain. Ductile crack advance prior to unstable cleavage fracture, needs to be modelled in order to investigate the transition region.

Acknowledgements

Financial support of Electricité de France is gratefully acknowledged.

References

- [1] Server W.L., "Charpy Impact Testing", ASM Handbook **Vol. 8**, American Society for Metals, 1985, 261-268.
- [2] Herzberg R., Deformation and Fracture Mechanics of Engineering Materials, 4th Edition, J. Wiley, New York (USA), 1995, 390-399.
- [3] Beremin F.M., *Met. Trans. A* **14A** (1983), 2277-2287.
- [4] Tahar M. and Piques R., "Résilience et ténacité d'un acier de cuve REP : rôle des veines sombres et des effets d'irradiation", Internal report Ecole des Mines de Paris (France), October 1995.
- [5] ABAQUS / Standard, Version 5.4, Theory Manual and User's Manual, Hibbitt, Karlsson & Sorensen, Inc., Pawtucket, RI, USA, 1994.
- [6] Giovanola H.J., "One-Point Test", ASM Handbook **Vol. 8**, American Society for Metals, 1985, 271-275.
- [7] Böhme W., "Dynamic Key-Curves for Brittle Fracture Impact Tests and Establishment of a Transition Time", in Fracture Mechanics : Twenty-First Symposium, ASTM STP 1074, 1990, 144-156.
- [8] Kalthoff J.F., "Concept of Impact Response Curves", ASM Handbook **Vol. 8**, American Society for Metals, 1985, 269-271.
- [9] Server W.L., *JTEVA* **6**, No. 1, Jan. 1978, 29-34.
- [10] Rossoll A., Berdin C., Forget P., Prioul C. and Marini B., "Mechanical Aspects of the Charpy Impact Test" Proceedings of ECF 11, Poitiers (France), 3-6 September 1996, 1933-1938.
- [11] Tahar M., Piques R. and Forget P., "Modelling of the Charpy-V Notch Test at Low Temperature for Structural Steels", Proceedings of ECF 11, Poitiers (France), 3-6 September 1996, 1945-1950.
- [12] Khalili A. and Kromp K., *J^{al} of Mat. Science* **26**, (1991), 6741-6752.
- [13] Di Fant M., Le Coq V., Cleizergues O., Carollo G., Mudry F., Bauvineau L., Burlet H., Pineau A., Marini B., Koundy M., Sainte-Catherine C., Eripret C., "Development of a Simplified Approach for Using the Local Approach to Fracture", this conference.